TWO-CHIP WIRELESS H_2S GAS SENSOR SYSTEM REQUIRING ZERO ADDITIONAL ELECTRONIC COMPONENTS

David C. Burnett, Hossain M. Fahad, Lydia Lee, Filip Maksimovic, Brad Wheeler, Osama Khan, Ali Javey, and Kristofer S. J. Pister
Berkeley Sensor and Actuator Center, Department of EECS, University of California, Berkeley

ABSTRACT

We describe a wireless hydrogen sulfide (H_2S) gas sensor system comprised of two integrated circuits: a chemically-sensitive field effect transistor (CS-FET) sensor and a single-chip micro-mote (SCμM). The sensor IC is a bulk transistor functionalized to respond to H_2S. The SCμM IC uses an ARM Cortex M0 to digitize sensor voltage via an ADC and transmit data through a 2.4GHz FSK transmitter based on an ultra-small, crystal-free, free-running ring oscillator. The IC pair has combined volume <4mm^3, requires only a power source & antenna and no additional components, and has been demonstrated to acquire signals resulting from H_2S gas and wirelessly transmit results at 2.4GHz.

KEYWORDS

Chemical sensor, hydrogen sulfide (H_2S), crystal-free wireless, sensor system, smart dust, internet of things.

INTRODUCTION

Advances in fabrication techniques have allowed great reductions in sensor size. However, when a sensor is integrated into a larger system, the control, readout, and communication electronics can dwarf the sensor itself [1] putting a high floor on size (1cm x 1cm x 0.2cm or more), power consumption (>20mW), and cost (>$10). Even when commercial sensors integrate digitizing & readout electronics inside the sensor package, communication still requires a wireless module. These modules are the driver for the size/power/cost limits above and include an RF IC, 1-2 crystal oscillators, passives, and sometimes an antenna, mounted on a PCB.

Surpassing these limitations could enable unobtrusive measurement of physiological signals [2] or wearable sensor tags to identify hazards in the environment at per-person spatial resolution. One such hazard is hydrogen sulfide gas (H_2S) with a recommended maximum exposure limit of 10ppm for 10 minutes and is immediately dangerous at concentrations above 100ppm [3]. This highly toxic gas is the example molecule we use to demonstrate this work, which combines control, readout, and communication electronics into a single IC to break through the aforementioned limits and enable ubiquitous and inexpensive environmental monitoring.

PROPOSED SYSTEM

Overview

We demonstrate a complete H_2S gas sensor system consisting of only a chemical sensor IC and a single-chip micro-mote (SCμM) ADC/CPU/wireless transmitter IC requiring only a power source and antenna to operate and offering a higher level of integration compared to existing chip-scale sensing and communication systems [4]. The sensor IC is a chemically-sensitive FET (CS-FET): a bulk NMOS transistor controlled by gas molecules adsorbing on the gate [5]. Such a transistor was functionalized to respond to H_2S through a Au layer added to the gate and connected to the external sensor pad of the single-chip mote. The CS-FET was fabricated via custom process and SCμM was fabricated in standard TSMC 65nm CMOS. A connection diagram is given in Fig. 1.

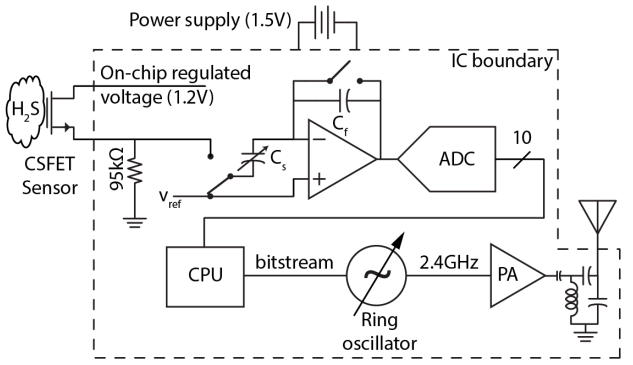

Figure 1: Schematic of CS-FET H_2S sensor connections to Single-Chip Micro-Mote (SCμM) sensor frontend between on-chip voltage source and resistor, and major blocks of SCμM processing & RF transmitter system.

Operation

When power is applied, the mote biases the CS-FET through regulated voltage and a static resistor. The presence of H_2S on the CS-FET Au catalyst layer allows more current flow between source and drain in the same manner as raising gate voltage in a traditional NMOS transistor. This increased current flow develops a higher voltage on the static 95kΩ resistor, which is amplified by the PGA by a factor of 2 and digitized by the 10-bit successive approximation register (SAR) ADC.

Software running on the on-chip ARM Cortex M0 CPU software controls power to the CS-FET, sets the PGA gain factor, triggers the ADC acquisition, and reads the result. Software then assembles the ADC result into a packet and transmits it by adjusting the current source of an RF oscillator to affect frequency shift keying (FSK) modulation. The oscillator is a current-starved, free-running, 8-stage 2.4GHz differential ring oscillator requiring no external crystal reference and its output is amplified by a switching power amplifier (PA).

Sensor bias and amplification

CS-FET devices are expected to allow 1μA current flow at 5ppm H_2S concentration [5] (half the NIOSH recommended exposure limit [3]). Bulk CS-FETs are, ideally, biased with a minimum 1V source-drain voltage

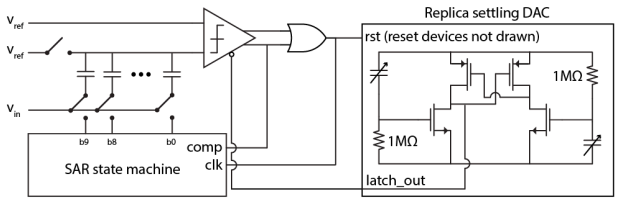

Figure 2: Schematic of self-timed ADC. After microprocessor triggers SAR state machine, each binary search occurs after comparator reset delay and replica settling DAC delay. Note: ADC reference voltage V_{ref} pictured here is different than PGA V_{ref} in Fig. 1.

during operation [6]. SCµM generates a 1.2V sensor voltage and the current at 5ppm H_2S concentration is expected to develop 95mV across the static resistor, leaving 1.105mV to bias the CS-FET.

The developed voltage is amplified by a switched-capacitor programmable gain amplifiers (PGA). These typically use reference voltage of zero and, as a result, the voltage gain is simply the ratio of the sampling capacitor and feedback capacitor (C_s/C_f). We use nonzero V_{ref} in our system so the expression for the PGA output voltage is:

$$V_{out} = \frac{C_s}{C_f} V_{in} + \left(\frac{C_s}{C_f} - 1 \right) V_{ref} \quad (1)$$

The sampling capacitor C_s is programmable between 1x and 256x larger than the feedback capacitor C_f. From this expression and with a nominal V_{ref} of 190mV generated on-chip, we can set amplifier gain (C_s/C_f ratio) to 2 and obtain a minimum V_{in}=95mV, above which V_{out} will be nonzero. This sets the minimum detectable input voltage to 95mV. At our H_2S target detection floor of 5ppm, the expected 1µA current is will develop 95mV across the static 95kΩ resistor and increase with higher gas concentration. Beyond approximately 10ppm, the source-drain voltage across the CS-FET will go below the recommended minimum. In this region of operation, the sensor remains responsive to increasing concentrations but at diminishing sensitivity and eventual railing of the input PGA voltage. This is acceptable behavior for our application, in which any detected concentration beyond 10ppm should result in immediate action to alleviate danger of H_2S poisoning.

Digital sampling

The PGA output connects to the ADC input. We take 200 ADC readings to average out thermal noise of the PGA reference voltage. ADC acquisition is split into three phases. During the first phase, the switched-capacitor PGA sampling capacitor is connected to *Vin* and the ADC is in reset. During the second phase, the PGA amplifies the sampled voltage and fills the ADC capacitor array. During the third phase, the ADC performs the conversion using internally-generated clocks and asserts an output when done. The CPU waits in a loop for the output to be asserted and reads the binary value from the SAR state machine.

The ADC design (Fig. 2) is based on [7] and adds a comparator input settling timer via a replica DAC [8]. The replica DAC output is connected to the state machine to generate binary search clocks internally instead of requiring an external clock. A digital OR gate is used to prevent slowdown in case of very close comparator inputs which would result in high comparator delay [9]. The replica DAC is adjustable to produce overall ADC conversion times from 0.35µs to 1.72µs.

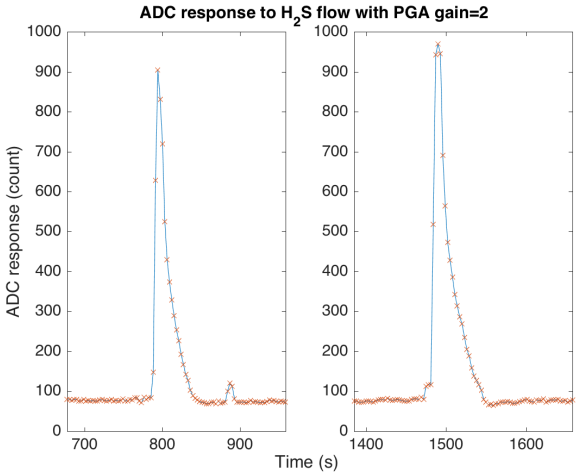

Figure 3: ADC values in response to two 10ppm H_2S flows (one short, one long) directed at Sensor A. Data points are marked with a red 'x' and were taken every 3 s.

Wireless Communication

On-chip software assembles the average of 200 ADC reading into a packet prepended with a Bluetooth LE-style preamble (0x07555555) and appended with a postscript (0x5533FF00) to assist a receiver in recovering data clock and recognizing the packet, respectively.

After assembling the packet, the CPU periodically adjusts the current source of the 2.4GHz ring oscillator to shift its frequency high or low depending on whether the next bit in the packet is a 1 or a 0. The separation between the "1" and "0" frequencies is typically small and changes fast because of the stability of crystal references. A calibrated crystal-free radio is still able to interoperate with standards-compliant wireless devices if it is based on a resonant LC tank oscillator [10]. Ring oscillators, which are smaller than LC tanks and can also benefit from future reductions in transistor size, exhibit higher frequency variance which requires us to exaggerate the typical FSK frequency separations found in wireless standards. For instance, the IEEE 802.15.4 standard uses a frequency shift of +/- 0.5MHz and a 0.5µs data period.

Literature indicates a free-running ring with approximately 500kHz jitter at 1ms intervals can achieve good communication performance (which we define as <1% packet error rate, or PER) using frequency shift of +/- 1MHz and a 0.5µs data period [11]. The ring in this work has 1.52MHz simulated jitter at 1ms intervals so we expect to need to increase frequency shift to +/- 3MHz.

EXPERIMENTAL RESULTS

System Operation

Two CS-FET sensors were tested in conjunction with the SCµM IC: Sensor A was tested with 10ppm H_2S flow and Sensor B was tested with 50ppm. Tests consisted of industry-standard "bump" tests conducted by briefly

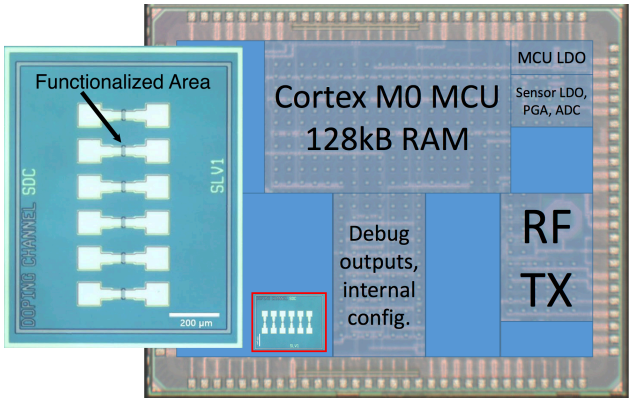

Figure. 4: Right: die photo of Single-Chip Micro-Mote (SCµM) IC measuring 2.5mm x 3mm including microprocessor, RAM, sensor interface, and reference-free 2.4GHz RF transmitter. Lower center, red outline: CS-FET IC pictured at scale with respect to SCµM IC. Left: CS-FET IC at 4x larger-than-scale with one of six H_2S-sensitive functionalized areas indicated.

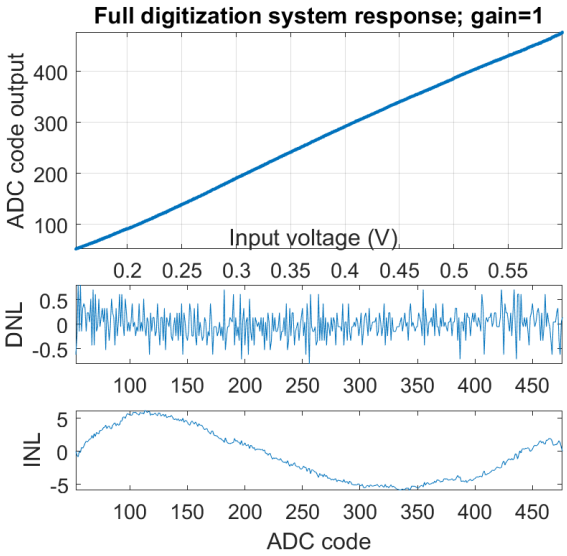

Figure 5: Voltage response of sensor frontend in region where system is least impacted by PGA/frontend nonlinearity and gain is set to unity. DNL extrema are [0.71, -0.81] and INL extrema are [5.4, -6.2].

flowing a pre-mixed concentration of H_2S gas and ambient air, waiting for the sensor to recover to baseline, and flowing gas again. All tests showed clear response. Continuous ADC readings for Sensor A are plotted in Fig. 3 indicating clear response to 10ppm. The first flow was terminated before the sensor reached steady state. The second flow lasted long enough to see a steady-state value before being terminated. Both took approximately 6 seconds to reach their peak value.

Of note is that the steady-state value during the second flow is the maximum ADC code reachable by this frontend. Given a PGA gain of 2, and accounting for nonlinearities at the top of the PGA range, this indicates current flow of at least 5.7µA through the fixed 95kΩ resistor. This is in excess of the 1µA estimated and, indeed, it was found that bulk devices are more sensitive than those in SOI [12]. This result has the effect of lowering our sensitivity floor by at least 5x which is beneficial for an ambient monitoring device: 10ppm is defined as the safe upper limit but long-term exposure to 2ppm is known to cause fatigue, headache, loss of appetite, and more [13]. In applications where these sensors are worn in everyday circumstances or many are distributed across a city, a lower detection floor is beneficial in preventing low-level exposure of an individual or population.

Photos of the ICs are shown in Fig. 4.

Data Acquisition

Each ADC conversion was measured to take 1.55µs but each acquisition cycle takes 337µs. The PGA is estimated to need at least 1.8µs to settle so the balance of time consists of software overhead required to, e.g., step the system through the three signal acquisition phases and store the result. We take 200 samples per data point for a total time of 67.4ms. The system response with PGA gain set to unity was obtained by incrementing V_{in} in 0.1mV steps and acquiring 30,000 measurements at each step. The results are plotted in Fig. 5.

The high DNL could indicate need for more thermal noise averaging, or a finer voltage step to more accurately determine ADC code boundaries. The wave-like plot of integral nonlinearity (INL) more clearly shows the same, opposite-phase, trend in the DNL. Its shape indicates low codes are represented by slightly more voltage than average and high codes are represented by slightly less. Fortunately our application does not demand high fidelity ADC performance and, worst-case, a lookup table to could be employed to compensate for these nonlinearities.

Data Transmission

Data was transmitted at a center frequency of 2.465GHz with an output power of –12dBm. A sample transmission is plotted in Fig. 6 showing FSK-modulated data. Considerably more random frequency error (phase noise and jitter) was observed in the RF carrier due to a significant underestimation of flicker noise in the simulation models. The RF carrier was modulated by approximately +/-7MHz to ensure high and low frequency shifts can be clearly distinguished. This necessity had an impact on data rate because the response time of the current DAC – which is responsible for FSK frequency shifts – is limited. A 249µs bit period was necessary to allow ample settling time for a 7MHz frequency shift. This means our proposed 12 byte packet takes 29.3ms to transmit. When added to the 67.4ms sensor sampling duration and compared with our overall 3 second sensor sampling period, we can expect a 3.0% duty cycle.

Power Consumption

The sensor, PGA, and ADC together consume 195µA from a 1.2V on-chip supply. The rest of the acquisition system including CPU, clocks, and voltage regulation consumes 604µA from a 0.8V on-chip supply. The free-running oscillator and power amplifier consume 1.08mA and 1.30mA from 1.2V, respectively, generated off-chip for experimental flexibility. Added together, the system consumes peak power of 0.71mW while sensing/acquiring and 2.85mW while transmitting. These values increase to

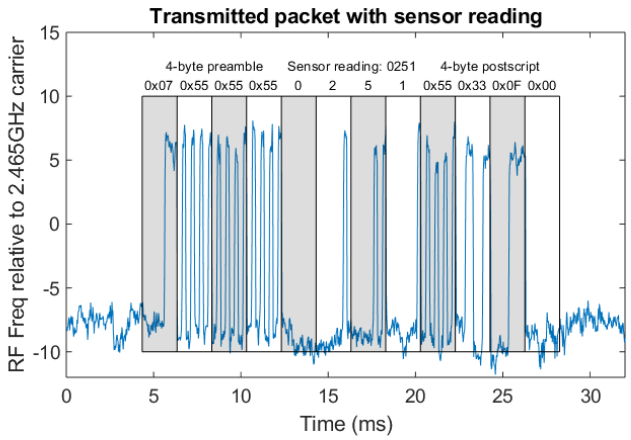

Figure 6: Wireless transmission of acquired sensor value during 50ppm H_2S flow over Sensor B.

1.20mW and 3.57mW, respectively, if we assume supply voltages are regulated from a 1.5V battery. With 3.0% duty cycle and assuming a future version of our system consumes typical 1µA while asleep, we can expect 188µW average power and 358 hours (>2 weeks) of lifetime from a 45mAh SR41 Ag_2O button cell battery.

CONCLUSIONS AND FUTURE WORK

We have demonstrated a complete wireless hydrogen sulfide sensor consisting of sensor IC and sensor acquisition/communication IC and requiring only antenna and power source to operate. The system is clearly responsive to H_2S gas concentrations at the NIOSH recommended exposure limit. Performance is acceptable for our application but several design improvement opportunities were made clear during testing.

Software overhead is responsible for 99% of time taken and power consumed while taking a sensor reading. This underscores the need for hardware control instead.

Shifting frequency by changing ring oscillator current turned out to be unnecessarily slow. Instead, a tunable capacitive DAC could be attached to the ring oscillator to adjust ring oscillator capacitive load, and therefore frequency, rapidly. This could be done on the order of 1µs, compared to this chip's 249µs limitation. This would also allow current DAC noise to be more aggressively filtered. Nominal power consumption would increase due to capacitive DAC parasitic loading but the results would be, in our opinion, well worth it given poor noise models.

Improved flicker noise models are clearly needed to allow minimum frequency shifts to be more accurately estimated in simulation. Tighter frequency spacing would reduce occupied bandwidth and increase the number of sensors capable of communicating in the 2.4GHz band.

With these straightforward improvements to shorten sensor readings to 3.5µs and packet transmission to 96µs, we estimate duty cycle could be as low as 0.2% yielding an average power of 5.6µW. Note the assumed 1µA sleep current is responsible for 53% of power consumed in this case. But even without such improvements, average power of 188µA paired with a scavenged energy source would enable unobtrusive, self-powered wearable toxic gas detection or cheap ubiquitously-distributable sensors capable of reporting dangerous conditions immediately.

ACKNOWLEDGEMENTS

Thanks to Niharika Gupta for assistance with experiments. This work was supported by the National Defense Science and Engineering Graduate (NDSEG) Fellowship and through the Berkeley Sensor and Actuator Center (BSAC).

REFERENCES

[1] W. Gao et al., "Fully integrated wearable sensor arrays for multiplexed in situ perspiration analysis," Nature, vol. 529, no. 7587, pp. 509–514, Jan. 2016.

[2] D. C. Burnett, B. L. Smarr, S. M. Mesri, L. J. Kriegsfeld, and K. S. J. Pister, "Reconfigurable, Wearable Sensors to Enable Long-duration Circadian Biomedical Studies," in Proceedings of the 9th International Conference on Body Area Networks, ICST, Brussels, Belgium, 2014, pp. 142–146.

[3] National Institute for Occupational Safety and Health, "NIOSH pocket guide to chemical hazards," U.S. Dept. of Health and Human Services (NIOSH) Publication No. 2005-149, p. 160, Sep. 2007.

[4] Y. Shi et al., "A 10 mm^3 Inductive Coupling Radio for Syringe-Implantable Smart Sensor Nodes," IEEE JSSC, vol. 51, no. 11, pp. 2570–2583, Nov. 2016.

[5] H. M. Fahad et al., "Room temperature multiplexed gas sensing using chemical-sensitive 3.5-nm-thin silicon transistors," *Science Advances*, vol. 3, no. 3, Mar. 2017.

[6] H. M. Fahad et al., "Highly Sensitive Bulk Silicon Chemical Sensors with Sub-5 nm Thin Charge Inversion Layers," ACS Nano, vol. 12, no. 3, pp. 2948–2954, Mar. 2018.

[7] M. D. Scott, B. E. Boser, and K. S. J. Pister, "An ultralow-energy ADC for Smart Dust," IEEE JSSC, vol. 38, no. 7, pp. 1123–1129, Jul. 2003.

[8] R. Kapusta, J. Shen, S. Decker, H. Li, E. Ibaragi, and H. Zhu, "A 14b 80 MS/s SAR ADC With 73.6 dB SNDR in 65 nm CMOS," IEEE JSSC, vol. 48, no. 12, pp. 3059–3066, Dec. 2013.

[9] P. J. A. Harpe et al., "A 26µW 8 bit 10 MS/s Asynchronous SAR ADC for Low Energy Radios," IEEE Journal of Solid-State Circuits, vol. 46, no. 7, pp. 1585–1595, Jul. 2011.

[10] F. Maksimovic et al, "A Crystal-Free Single-Chip Micro Mote with Integrated 802.15.4 Compatible Transceiver, sub-mW BLE Compatible Beacon Transmitter, and Cortex M0," in 2019 Symposium on VLSI Circuits, 2019, *to appear*.

[11] D. C. Burnett et al., "Narrowband communication with free-running 2.4GHz ring oscillators," in IEEE PEMWN 2017, pp. 1–6.

[12] H. M. Fahad et al., *in review*.

[13] J. Lindenmann et al, "Severe hydrogen sulphide poisoning treated with 4-dimethylaminophenol and hyperbaric oxygen." Diving and Hyperbaric Medicine. 40 (4): pp. 213–217, December 2010, PMID: 23111938.

CONTACT

David C. Burnett, db@eecs.berkeley.edu